2022

Evaluation of the Lubrication Regime for Rotary Compressors. Influence of Thermal Expansions on the Minimum Film Thickness.

Jordi Vera

Eugenio Schillaci

Joaquim Rigola

Evaluation of the lubrication regime for rotary compressors. Influence of thermal expansions on the minimum film thickness.

Jordi VERA[1], Eugenio SCHILLACI[2*], Joaquim RIGOLA[1]

[1] Universitat Politècnica de Catalunya - Barcelona Tech (UPC),
ESEIAAT, C/ Colom, 11 - 08222 Terrassa (Barcelona), Spain

[2] Termo Fluids S.L.,
Carrer Magi Colet 8, Sabadell (Barcelona), Spain

* Corresponding Author (eugenio@termofluids.com)

ABSTRACT

In this work, the lubrication regime of a rotary compressor is studied in the regions of the roller, cylinder, shaft, and bearings. A code is programmed so it can solve multiple cases with different suction-discharge pressures, angular velocity, viscosity, and geometrical conditions, among others. In order to study the lubrication regime, the balance of the different forces that act on the roller is computed. To calculate the oil pressure forces, the Reynolds equation coupled with an iterative method is used to find the minimal distance and pressure distribution that balances the external forces. This process is repeated for a discrete number of rotation angles to evaluate the overall rotation of a cycle. In addition, the effect that the thermal expansion of the different materials can have on the lubrication regime is studied. If the materials get too hot, the distances between surfaces might increase or reduce with respect to the distances at room temperature. These changes might lead to a point where the lubrication regime changes. The objective is to include this thermal expansion effect in the model and evaluate how it can affect the lubrication regime.

1. INTRODUCTION

The rotary compressor is an element that compresses a refrigerant using rotary motion. An oil that is mixed with the refrigerant is used to lubricate moving parts. A simplified diagram of the rotary compressor and studied lubricated contact surfaces is shown in Figure 1.

The objective of this work is to create a model capable of studying the lubrication regime of a rotary compressor. This lubrication regime depends mainly on the forces acting on the compressor, the geometry, the rotating speed, and the oil viscosity. Other parameters also play an important role in the model. Several models have been made regarding the study of the lubrication regime between surfaces. A common and simple approach is to use the curves developed by (Raimondi & Boyd, 1958). These curves can give the minimum film thickness given a force and some geometrical and operational parameters. Another approach is to compute the forces and numerically solve the Reynolds equation for each case and determine the lubrication regime. Some examples of this approach are shown in (Ito, Hattori, & Miura, 2010), (Zhou, 2012) and (Noh et al., 2016), among others. The complexity and accuracy of these types of models is increased by adding more parameters. For example in (Mi & Meng, 2014) the movement of the roller is also evaluated with the equations of motion.

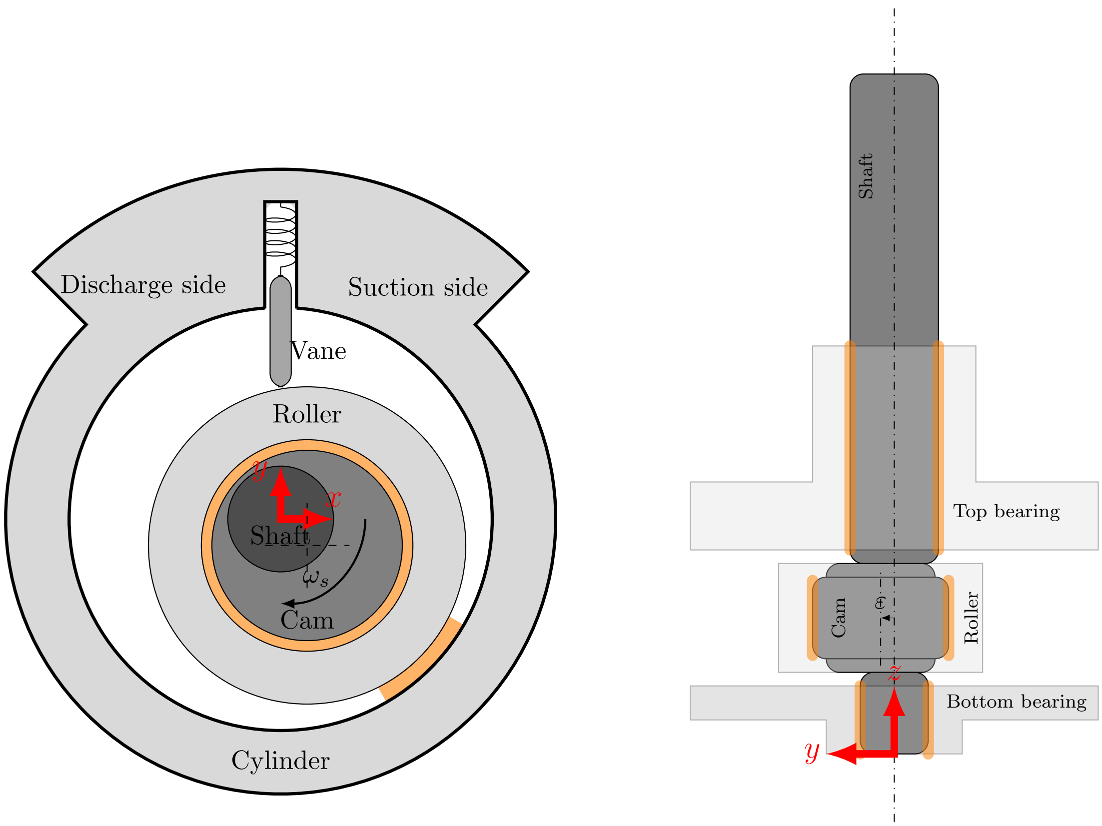

(a) Rotary compressor geometry, front view **(b)** Shaft and cam contact surfaces

Figure 1: Rotary compressor geometry and lubricated parts

The main idea is that the pressure force of the oil compensates for the acting forces, however, as the force increases, the distance between surfaces decreases and the regime of lubrication might change, as shown in Figure 2.

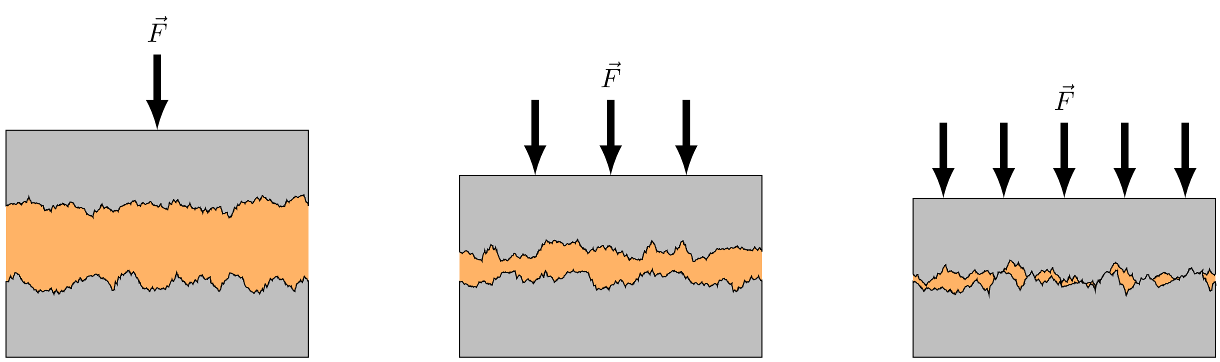

Hydrodynamic lubrication $\Lambda > 3$ Mixed lubrication $\Lambda \sim 1 - 3$ Boundary lubrication $\Lambda < 1$

Figure 2: Oil lubrication and film thickness for different loads

The regime of lubrication is defined as the relation between the minimum film thickness and the surface rugosity $\mathcal{R}$ of each surface.

$$\Lambda = h_{\min}/\sqrt{\mathcal{R}_1^2 + \mathcal{R}_2^2} \tag{1}$$

The chosen approach considers a known roller movement, and the balance of forces at the roller, shaft, and bearings is used to determine the minimum film thickness by solving the Reynolds equations. Using the developed model, a parametric study is carried out to study the influence of thermal expansions in the lubrication regime.

The calculations are performed for each angle of rotation θ. This angle corresponds to the rotation position of the shaft. The definition of this angle is shown in Figure 3

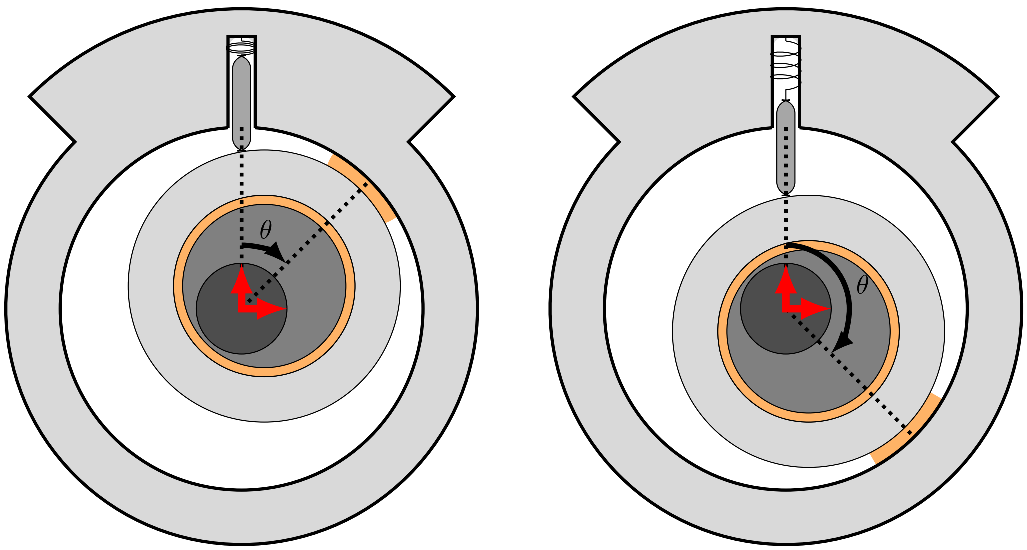

Figure 3: Shaft angle θ definition

The paper is distributes as follows: the numerical set-up is described in Sec. 2, the algorithm is explained in Sec. 3, then an example test case is shown in Sec. 4, finally this case is modified to evaluate the influence of thermal expansions at 4.2.

2. NUMERICAL SET-UP

The objective is to evaluate the lubrication regime for each studied contact surface. The first step for each surface is to solve its pressure distribution a given $h_{\min}/c$ value. This is done solving the Reynolds Equation (Section 2.1). This pressure distribution has to be integrated to obtain the reacting force. The process is repeated for multiple $h_{\min}/c$, obtaining a curve of the force as a function of the eccentric displacement $F(h_{\min})$. Then performing a force balance, as shown in Section 2.2, the minimum film thickness can be found for each rotation angle θ.

2.1 Reynolds equation

The Reynolds equation (2) gives us the pressure distribution.

$$\nabla \cdot \left(\frac{h^3}{\mu} \nabla p \right) = 6\Omega \frac{\partial h}{\partial \theta'} \tag{2}$$

Where h is the distance between surfaces at a given position, p the pressure, μ the viscosity, and Ω the relative angular velocity between surfaces.

To solve the equations, they are discretized using the finite volume method, using the 2D Gauss theorem.

$$\int_S \nabla \cdot \left(\frac{h^3}{\mu} \nabla p \right) \, dS = \int_S 6\Omega \frac{\partial h}{\partial \theta'} \, dS \qquad \rightarrow \qquad \int_{\mathcal{C}} \frac{h^3}{\mu} \nabla p \cdot \vec{n} \, d\mathcal{C} = \int_S 6\Omega \frac{\partial h}{\partial \theta'} \, dS \tag{3}$$

Considering the discrete form we have:

$$\frac{h_e^3}{\mu} \frac{p_{i+1,j} - p_{i,j}}{\Delta z'^2} + \frac{h_w^3}{\mu} \frac{p_{i-1,j} - p_{i,j}}{\Delta z'^2} + \frac{h_n^3}{\mu} \frac{p_{i,j+1} - p_{i,j}}{(R\Delta\theta')^2} + \frac{h_s^3}{\mu} \frac{p_{i,j-1} - p_{i,j}}{(R\Delta\theta')^2} = 6\Omega \frac{\partial h}{\partial \theta'} \tag{4}$$

Given a $N_\theta \times N_z$ mesh, Expression (4) gives a $N_\theta \times N_z$ linear system of equations that can be solved using a linear solver (e.g. Gauss-Seidel).

A special case has to be considered in the solution for the system of equations, when the pressure gives negative values, the solution at that point is non-physical. In general, this zone is considered a cavitation zone, so the pressure will be artificially threshold to only positive values and set to zero negative values, as shown in Figure 4.

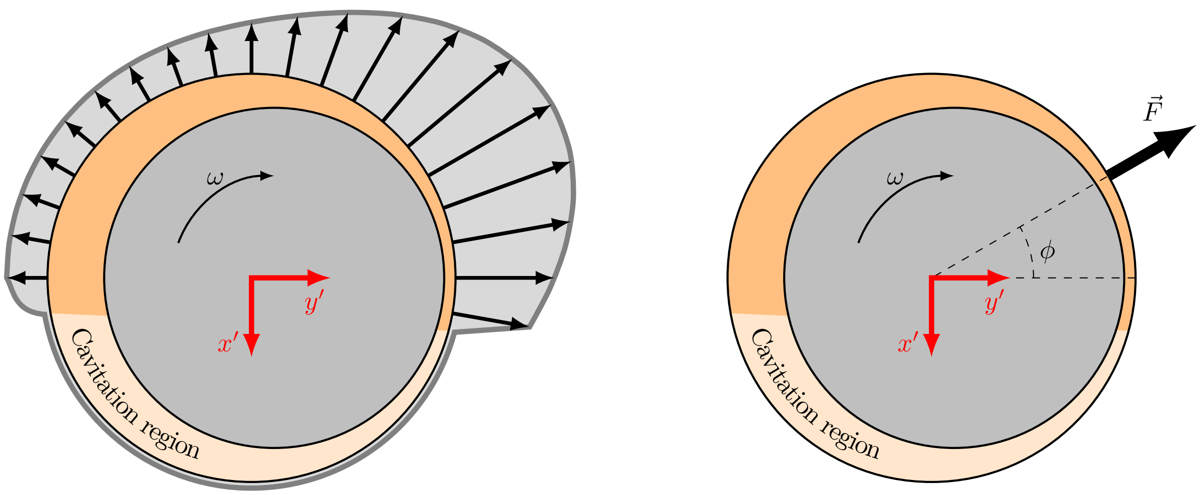

Figure 4: Pressure distribution (left) and global force and angle with respect to h_{min} (right)

The solution of the Reynolds equations give us a pressure distribution field on the surface as shown in Figure 5.

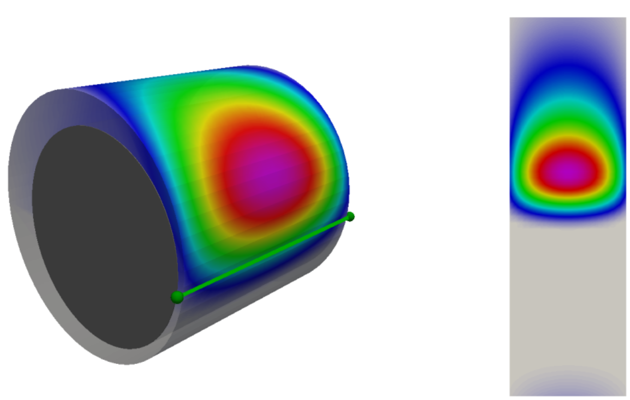

Figure 5: Pressure distribution field for a bearing. The line indicates the minimum film thickness position.

2.2 Force balances

In order to calculate the pressure force of the refrigerant, the pressure is integrated over all the surface. The pressure at the suction chamber is considered constant. The pressure at the discharge chamber is a function of the instantaneous chamber volume, which is a function of the shaft angle θ.

$$P_2(\theta) = P_s \left(\frac{V_{\theta_0}}{V_\theta}\right)^k \qquad \text{if } P_2 < P_d \tag{5}$$

$$P_2(\theta) = P_d \qquad \text{otherwise} \tag{6}$$

Where P_s is the suction pressure, P_d the discharge pressure, V_{θ_0} is the volume of the chamber at the initial position ($\theta = 0$), V_θ is the volume of the chamber at the current position, and k is the Polytropic compression exponent of the refrigerant.

The normal vane force can be easily calculated using Hooke's law.

$$\vec{F}_{\text{vane}} = -k \cdot \Delta x \tag{7}$$

The inertial force $\vec{F}_I^r$ is given by the angular velocity, mass and eccentricity.

Finally the reaction force is unknown, but can be obtained with the summation of all the other forces.

$$\vec{F_R} = -\left(\vec{F}_{\text{vane}} + \vec{F}_{P1} + \vec{F}_{P2} + \vec{F_{oil}} + \vec{F}_I^r\right) \tag{8}$$

Having the roller force, the reaction force of the bottom and top bearings can be calculated as follows:

$$\vec{F}_b + \vec{F}_t = \vec{F}_I^{cm} - \vec{F_R} \tag{9}$$

A diagram of acting forces is shown in Figure 6.

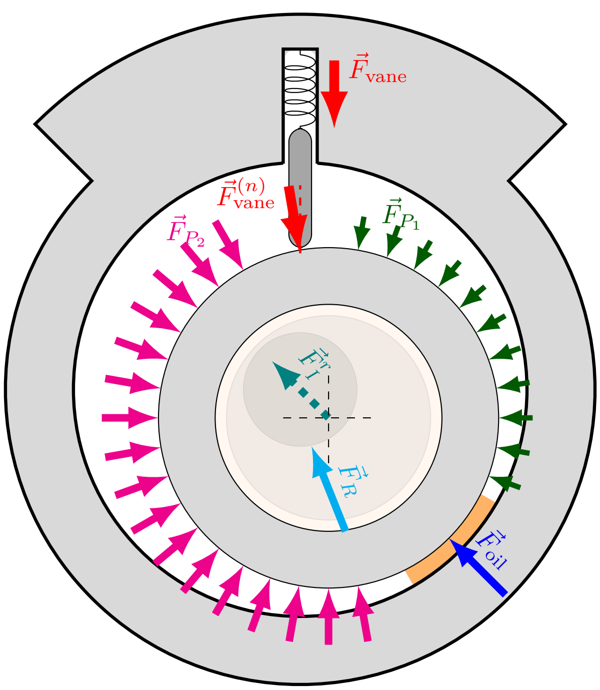

(a) Forces acting on the Roller

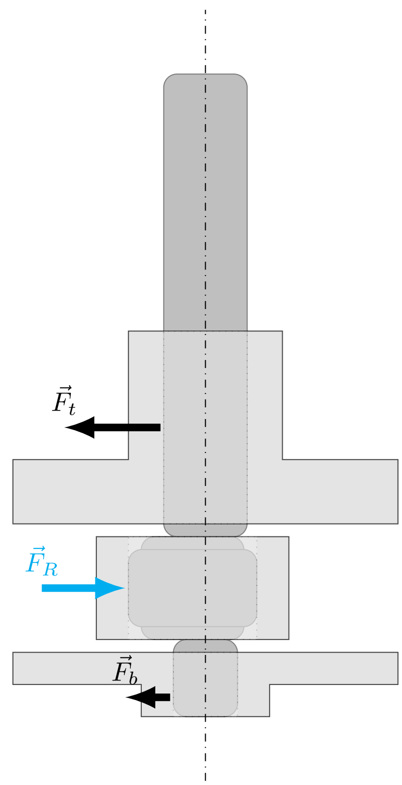

(b) Shaft applied forces

Figure 6: Acting forces on the rotary compressor

2.3 Roller dynamics

The shaft movement is an imposed parameter, it consists of a rotation along its axis characterized by the angle of rotation θ. It will rotate at a given speed $\dot{\theta} = -\omega_s$. This speed is known.

The roller has two degrees of freedom, one would be the angle θ (shaft rotation) and the other would be an angle ψ (angle between the roller and the shaft). The evolution of this parameter ψ is unknown and will depend on the forces acting on the roller. We will call the angular speed of the roller $\dot{\psi} = -\omega_r$.

The proper way to determine the roller movement would be to formulate the movement equations, solve this equations numerically, and get $\psi(t), \dot{\psi}(t), \ddot{\psi}(t)$. However the oil film forces are also unknown, and they depend on the roller movement, so we would have to make a coupled solver that solves the movement and the forces together. This is possible and could be archived using iterative methods, as it is done in (Mi & Meng, 2014), however, this would increase the complexity of the code and formulation, so this approach is discarded.

From some papers that performed numerically and experimental analysis (Yanagisawa, Shimizu, Chu, & Ishijima, 1982) regarding the roller movement, we can conclude that we will have at most $\omega_r \approx \pm 0.1\omega_s$ depending on the angle and the dynamics. To simplify the model and avoid solving the equations of motion of the roller, which would lead to the need of coupling the movement with the Reynolds equations and do an iterative algorithm, we will consider that the roller angular velocity $\omega_r = 0$. The relative velocity between the roller and the shaft will be ω_s (Shaft angular velocity).

3. ALGORITHM

A first preprocess described in Algorithm 1 is performed for each lubrication surface. This will save the acting force as a function of the displacement on a bearing solving the Reynolds equations.

Algorithm 1 Finding $S(h_{min})$ curves

```
Start in equilibrium condition (displacement δ = 0)
while δ < 1 do
    Solve the Reynolds equations to get the pressure distribution p(θ', z)
    Integrate the pressure distribution to get the force F(δ) and angle φ(δ)
    Calculate Sommerfeld number
    Advance a displacement δ_i = δ_i + Δδ_i
end while
```

Then the main algorithm of the code is

Algorithm 2 Main algorithm

1: Input physical parameters
2: Input numerical parameters
3: Find $S(h_{min})$ for bottom bearing/shaft to save $F_1(\delta_1)$ and $\phi_1(\delta_1)$
4: Find $S(h_{min})$ for top bearing/shaft to save $F_2(\delta_2)$ and $\phi_2(\delta_2)$
5: Find $S(h_{min})$ for the roller/cam to save $F_3(\delta_3)$ and $\phi_3(\delta_3)$
6: $\delta_i = \delta_i + \Delta\delta_i$
7: Join curves from bottom (line 3) and top (line 4) bearings into $\vec{F}_{12}(\delta_{12})$
8: $\theta = 0$
9: **while** $\theta < 360$ **do**
10: Calculate known acting forces ($\vec{F}_I^r$, $\vec{F}_I^{cm}$ $\vec{F}_{P1}$, $\vec{F}_{P2}$ and $\vec{F}_{\text{vane}}$)
11: Calculate roller force $\vec{F}_r$ and find δ_3 interpolating from $F_3(\delta_3)$ (line 5)
12: Calculate total bearing forces ($\vec{F}_b + \vec{F}_t$) and find δ_{12} interpolating from $F_{12}(\delta_{12})$ (line 7)
13: Decompose the bearing displacements $\delta_{12} \to \xi_{12} \to (\delta_1, \delta_2)$
14: Calculate bottom bearing force $\vec{F}_b$ interpolating from $F_1(\delta_1)$ (line 3)
15: Calculate top bearing force $\vec{F}_t$ interpolating from $F_2(\delta_2)$ (line 4)
16: Align the forces and find $\vec{\xi}_s, \vec{\xi}_{rs}, \vec{\xi}_r$
17: Calculate $\vec{F}_{\text{oil}}$ from $\vec{\xi}_r$ and verify is small enough (check hypothesis)
18: Store $\delta_{min(i)}$ and calculate the lubrication regime for each surface $\Lambda_{(i)}$
19: Print results
20: Advance the shaft angle $\theta = \theta + \Delta\theta$
21: **end while**
22: Print final results and post-processing

4. RESULTS

In this section first the results of a chosen reference case are shown. Then this same case but with the parametric variation is studied.

4.1 Reference case results

In Figure 7 the forces acting on the roller are presented. Figure 8 shows the lubrication curve for the Roller-Cam interface. Finally, Figure 9 shows the lubrication regime for the bottom bearing, top bearing, roller, and cylinder. As it can be observed, the main driving force is the pressure force.

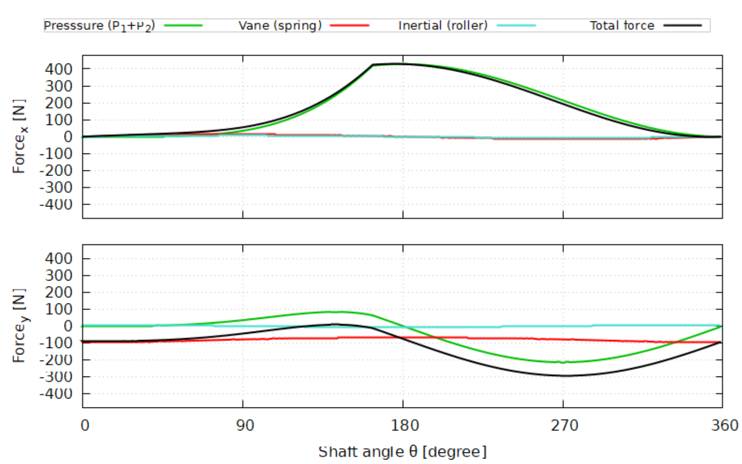

Figure 7: Acting forces on the roller as a function of the rotation angle

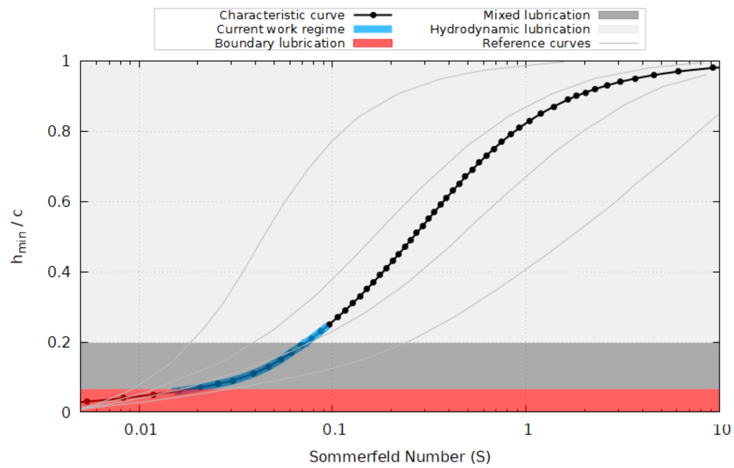

Figure 8: Lubrication regime Λ for the Roller-Cam interface

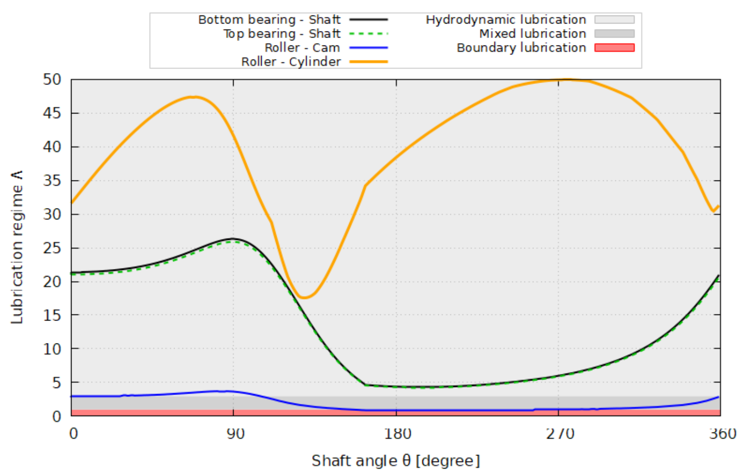

Figure 9: Lubrication regime Λ for the Roller-Cam interface

4.2 Parametric case results

For the Roller, made of a gray cast iron, a thermal expansion coefficient of $\alpha_2 = 10.5\ \mu\text{m}/(\text{m}^\circ\text{C})$ is considered. For the Shaft, made from a ductile cast iron, a thermal expansion coefficient of $\alpha_1 = 12\ \mu\text{m}/(\text{m}^\circ\text{C})$ is used. The changes of diameter due to temperature differences are given by equation (10)

$$L' = L(1 + \alpha\Delta T) \tag{10}$$

Let's assume that the Roller-Cam interface have a diameter of 20 mm with a clearance of 0.02 mm (20 μm)

Table 1: Clearance variation as a function of temperature

Temperature	Inner diameter D_1	Outer diameter D_2	Clearance c	c variation c/c_0
20 $^\circ C$	19.980 mm	20.000 mm	0.0200 mm	100 %
40 $^\circ C$	19.985 mm	20.004 mm	0.0192 mm	96 %
60 $^\circ C$	19.990 mm	20.008 mm	0.0185 mm	92 %
80 $^\circ C$	19.995 mm	20.012 mm	0.0177 mm	88 %
100 $^\circ C$	20.000 mm	20.017 mm	0.0170 mm	85 %

As shown in Table 1, in this case we could get a 15% reduction of the clearance distance. In the results shown in Table 2 the following changes of lubrication regime and friction forces are observed:

Table 2: Results of the lubrication regime Λ and friction force on the roller as a function of temperature

Temperature	Lubrication regime Λ	Friction force
20 $°C$	0.98	0.757 N
40 $°C$	1.00	0.767 N
60 $°C$	1.02	0.776 N
80 $°C$	1.05	0.786 N
100 $°C$	1.05	0.796 N

In this case in particular we observe that the lubrication regime improves from boundary lubrication ($\Lambda < 1$) to mixed lubrication. The changes are about 7%. We can also observe this behaviour in Figure 10. As the clearance decreases, the Sommerfeld number increases as it is proportional to $1/c^2$, so the working regime curve is displaced to the right. Even if the lubrication regime improves, we can observe that the friction force between the roller and cam increases up to a 5%. This simulation was performed for some specific conditions, so other conclusions might arise if testing another case, but the general conclusion is that the effect of thermal expansion is a parameter that will have some effect on the simulation results. For simplicity in most models it can be neglected, but including this variation would improve the accuracy without the need of increasing the computational cost or complexity of the model.

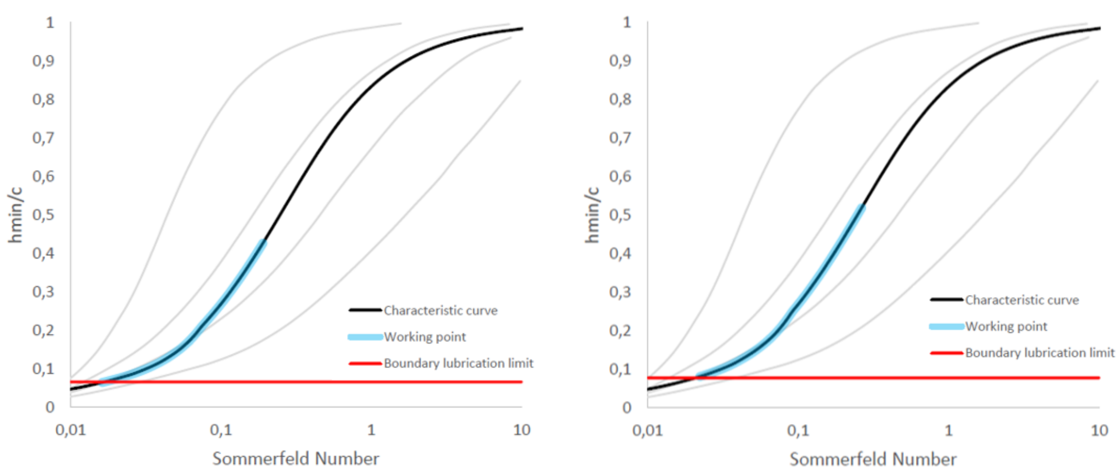

Figure 10: Change of working regime from thermal expansion between room temperature (left) and surfaces at 100 °C (right) keeping the rest of variables constant.

5. CONCLUSIONS

In general, the acting forces on the roller are mainly driven by pressure forces. Other forces are also considered but could be neglected if a simpler model was to be made. In the specific case studied case, it was observed that the increase in temperature improved the lubrication regime. This is because the smaller the clearance, the more pressure a bearing can support. However, even if the lubrication regime improves, an increase in the friction force was observed. In conclusion, the thermal expansion can have some effect on the lubrication regime and friction between surfaces, and its addition to the model can be done straightforwardly when assuming known and constant element temperatures.

REFERENCES

Ito, Y., Hattori, H., & Miura, K. (2010). Numerical analysis for rotating motion of a rolling piston in rotary compressors-effective factors for characteristics of rotating motion of a rolling piston.

Mi, J., & Meng, Y. (2014). Numerical analyses of hydrodynamic lubrication and dynamics of the rolling piston and crankshaft in a rotary compressor. *Tribology Transactions*, *57*(6), 1136–1147.

Noh, K.-Y., Min, B.-C., Song, S.-J., Yang, J.-S., Choi, G.-M., & Kim, D.-J. (2016). Compressor efficiency with cylinder slenderness ratio of rotary compressor at various compression ratios. *International journal of refrigeration*, *70*, 42–56.

Raimondi, A., & Boyd, J. (1958). A solution for the finite journal bearing and its application to analysis and design: Iii. *ASLE Transactions*, *1*(1), 194–209.

Yanagisawa, T., Shimizu, T., Chu, I., & Ishijima, K. (1982). Motion analysis of rolling piston in rotary compressor.

Zhou, X. (2012). Minimum viscosity for bearing reliability in r290 rotary compressors.

ACKNOWLEDGMENT

The author Jordi Vera has been financially supported by the Ministerio de Educación y Ciencia (MEC), Spain, (FPI grant PRE2018-084017). The author E.Schillaci acknowledges the financial support of the Programa Torres Quevedo (PTQ2018-010060).